JOURNAL OF PROPULSION AND POWER
Vol. 23, No. 4, July–August 2007

Friction Stir Welding of GRCop-84 for Combustion Chamber Liners

Carolyn K. Russell* and Robert Carter†
NASA Marshall Space Flight Center, Huntsville, Alabama 35812
David L. Ellis‡
NASA John H. Glenn Research Center at Lewis Field, Cleveland, Ohio 44111
and
Richard Goudy§
Spin Tech, Paso Robles, California 93446

DOI: 10.2514/1.11645

GRCop-84 is a copper-chromium-niobium alloy developed for liquid rocket engine combustion chamber liners. GRCop-84 exhibits superior properties over conventional copper-based alloys in a liquid hydrogen–oxygen operating environment. A program to demonstrate scale-up production capabilities of GRCop-84 to levels suitable for main combustion chamber production for the prototype rocket engine was undertaken. This paper describes a novel method of manufacturing the main combustion chamber liner. The process consists of several steps: extrude the GRCop-84 powder into billets, roll the billets into plates, bump form the plates into cylinder halves, and friction stir weld the halves into a cylinder. The cylinder is then metal spun formed to near net liner dimensions, followed by finish machining to the final configuration. This paper describes the friction stir weld process development, including tooling and nondestructive inspection techniques, culminating in the successful production of a liner preform completed through spin forming.

I. Introduction

THE copper-chromium-niobium (Cu-Cr-Nb) system was first examined for rocket engine applications under NASA's Earth-to-Orbit Program [1,2]. The goal was to develop a high thermal conductivity material with high tensile strength, long creep lives, and long low-cycle fatigue (LCF) lives. To reduce thermally induced stresses, a low coefficient of thermal expansion (CTE) was also desired.

Examination of the metallic elements showed that the four elements with the highest thermal conductivities were aluminum, gold, copper, and silver, in order of increasing thermal conductivity. Aluminum melts at too low a temperature to be useful, whereas gold is too dense for a rocket engine application. Of the two remaining elements, silver has only a slightly higher thermal conductivity than copper but melts 123°C (221°F) lower than copper. Based upon these considerations, copper was chosen as the base element.

To achieve a combination of high strength and conductivity, either dispersion strengthening or precipitation strengthening works best [3]. Precipitation strengthening was chosen as the primary strengthening mechanism for the alloy, for processing reasons. To further reduce the solubility of the secondary phase in the base element, a binary compound was desired. It was advantageous to have the compound's constituents have low solid solubility in copper but high solubility in liquid copper. Examination of the available binary and ternary phase diagrams revealed that chromium (Cr) and niobium (Nb) formed the high melting point intermetallic compound Cr_2Nb, had minimal solid solubility in solid copper, and were completely soluble in liquid copper.

Maximizing the volume fraction and minimizing the size of the Cr_2Nb secondary phase would maximize the strength of the alloy [4]. Rapid solidification processing such as chill block melt spinning and gas atomization can be used to form extended solid solutions from which a secondary phase such as Cr_2Nb can be precipitated [5]. The ribbon or powder produced can be consolidated by conventional powder metallurgy methods, and the consolidated material can be processed like other copper alloys.

In practice, it became evident that the vast majority of the Cr_2Nb precipitates in the liquid phase even with rapid solidification techniques. This led to dispersion strengthening instead of precipitation strengthening. This still gives the Cu-Cr-Nb alloys excellent strength while retaining a high thermal conductivity.

Based upon examination of alloys with Cr contents ranging from 2 to 10 atomic percent and Nb contents ranging from 1 to 5 atomic percent with a constant Cr:Nb ratio of 2:1 [6], the best combination of properties and processability appears to be obtained with 8 atomic percent Cr and 4 atomic percent Nb. This alloy was designated GRCop-84 and selected for further analysis and scale-up.

There are five major properties used to determine the suitability of an alloy for use in a regeneratively cooled rocket engine liner: tensile strength, creep resistance, low-cycle fatigue, thermal expansion, and thermal conductivity. Of the five, thermal conductivity and low-cycle fatigue or low-cycle fatigue–creep are generally the most important for designing a liner.

There are several copper-based engine liners in use, with several more proposed by various engine programs. The engine designs tend to use one of five alloys: pure copper, NARloy-Z (Cu 3 wt % Ag and 0.5 wt % Zr), GlidCop AL-15 (Cu 0.7 vol % Al_2O_3) or AL-60 (Cu 2.7 vol % Al_2O_3), and AMZIRC or zirconium copper (Cu 0.15 wt % Zr). The field is generally further reduced by the elimination of GlidCop AL-60, due to its 10% lower thermal conductivity relative to GlidCop AL-15 with little increase in other properties. In general, most comparisons are done to NARloy-Z, because it is the alloy currently in use for the main combustion chamber liner of the space shuttle main engine.

Presented at the 45th AIAA/ASME/ASCE/AHS/ASC Structures, Structural Dynamics, and Materials Conference, Palm Springs, CA, 19–22 April 2004; received 14 July 2004; revision received 25 July 2006; accepted for publication 1 September 2006.

*Aerospace Welding Engineer, Materials, Processes and Manufacturing, ED33.
†Aerospace Welding Engineer, Materials, Processes and Manufacturing, ED33.
‡Materials Research Engineer, MS49-1.
§President, 500 Linne Road, Unit F.

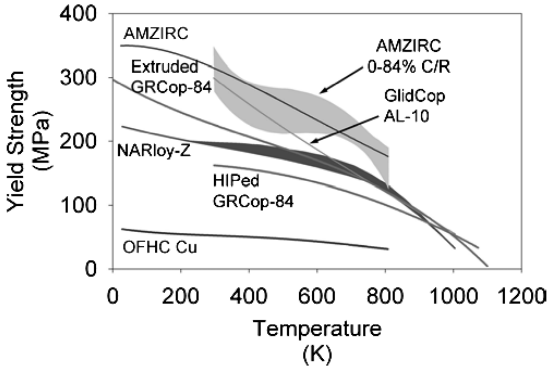

Fig. 1 Yield strength of candidate liner alloys (Cu [10], solution heat-treated and aged (STA) NARloy-Z [8], GlidCop AL-15 [8], and AMZIRC [8,10].

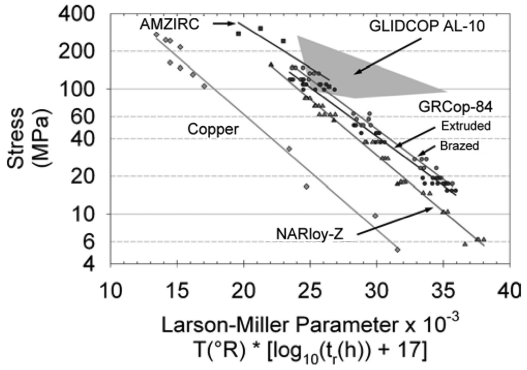

Fig. 3 Larson–Miller plot of creep lives of candidate liner alloys (copper [8], GlidCop AL-15 and AL-35 [12], AMZIRC [8], and NARloy-Z [11].

GRCop-84 powder has been consolidated by both extrusion and hot isostatic pressing (HIP). Both methods produced fully consolidated material. Samples from both consolidation techniques were given a simulated braze thermal cycle with a maximum temperature of 935°C (1715°F) to examine the stability of the alloy.

Figure 1 shows the yield strength of the various alloys in a variety of conditions. For alloys that have data taken from multiple sources, a range is shown that encompasses the values reported.

GRCop-84 given a HIP cycle is exposed to higher temperatures and undergoes more coarsening than the extruded GRCop-84. As a result, the yield strength is slightly lower. GRCop-84 has higher yield strengths than NARloy-Z over the entire temperature range of interest. The GlidCop alloys have higher yield strengths near room temperature, but the advantage disappears at elevated temperatures such as 500°C (932°F), the anticipated hot wall temperature of the liner. AMZIRC, which derives almost all of its strength from cold work, has higher yield strengths than as-produced (no cold work) GRCop-84.

Little open literature is available on the effect of high-temperature exposures such as one experienced in a brazing operation on these copper-based alloys. What data have been found for these alloys are shown in Fig. 2.

For copper, there should be little change in properties, because the material is already fully annealed, but there will be considerable grain growth, which may have limited deleterious effects. Increasing the grain size from 0.060 to 0.850 mm (0.002 to 0.033 in.) decreases the room-temperature yield strength 14 MPa (2 ksi) [7].

AMZIRC softens when exposed to temperatures between 350 and 600°C (572 and 1112°F) [8]. Following a 30-min exposure above 600°C, the room-temperature yield strength of AMZIRC decreases to approximately 250 MPa (36.2 ksi).

GlidCop AL-15 low oxygen grade has been tested following a 980°C (1796°F) simulated braze cycle and a 100-h anneal at 1040°C (1904°F) by Stephens et al [7]. The simulated braze cycle had little effect on the yield and ultimate tensile strengths, but did increase ductility slightly. The long-term, high-temperature annealed material, which resulted in considerable coarsening of the grains, reduced the yield strength to around 125 MPa (18.1 ksi), but enhanced ductility from 17.5 to 23.5% total elongation.

The effect of the high-temperature braze cycle on GRCop-84 depended upon the prior processing. The yield strength of extruded material, which was processed well below the braze temperature and experienced shorter thermal exposures during processing, decreased 21–35 MPa (3–5 ksi) across the temperature range tested. HIP material, which saw a long time at elevated temperatures during consolidation, was virtually unaffected. The excellent retention of properties following extended high-temperature exposures is one of the major benefits of GRCop-84.

Creep lives of the various materials come from a variety of sources and cover a wide range of temperatures and stresses. To compensate for these variations, the data were plotted on a Larson–Miller plot with the time to rupture in hours [t_r(h)] and the temperature in Rankine [T(°R)], using an assumed Larson–Miller parameter of $c = 17$ based upon prior experience with a variety of copper alloys. The actual value is not known for the alloys, but is expected to fall between 16 and 18. Although the limitations of the Larson–Miller analysis are recognized, the plot does allow for a semiquantitative comparison of the alloys' creep properties. The results are presented in Fig. 3.

Compared with the other alloys, GRCop-84 has excellent creep resistance. The creep life at a given stress can be increased by two or even three orders of magnitude over NARloy-Z. Alternatively, GRCop-84 can support 10–15% greater stresses for a given life than can NARloy-Z.

Low-cycle fatigue is generally considered the prime mechanical property for selecting a liner material. Figure 4 shows the low-cycle fatigue lives of several of the alloys. GlidCop AL-15 has poor LCF lives despite good strength and reasonable ductility. NARloy-Z has better LCF life, but the alloys with the best LCF properties are GRCop-84 and AMZIRC. The GRCop-84 LCF lives were virtually

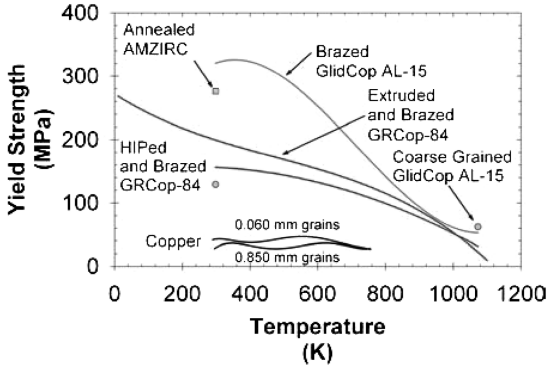

Fig. 2 Yield strength of candidate liner alloys following a high-temperature thermal exposure. Temperatures and times of exposure are Cu −350°C/30 min, Glidcop AL-15 −1040°C/100 h, AMZIRC −450°C/1 h (Cu [9], GlidCop AL-15 [7], and AMZIRC [10]).

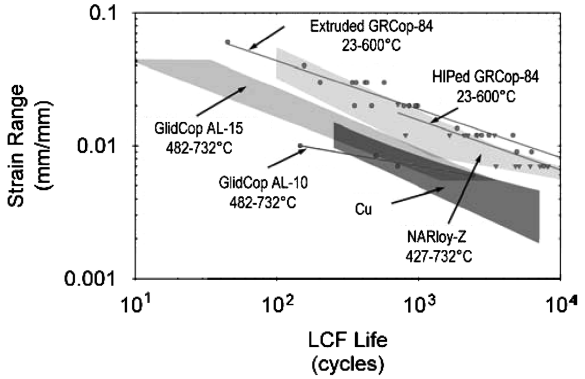

Fig. 4 Low-cycle fatigue lives of candidate liner alloys (copper [14,15], GlidCop AL-10 [16], GlidCop AL-15 [16], and NARloy-Z [17,18].

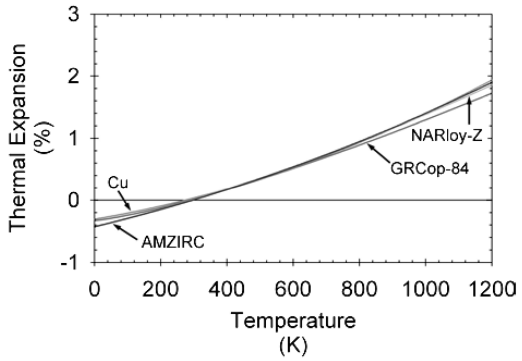

Fig. 5 Thermal expansion of candidate liner alloys (copper [19], AMZIRC [8], GRCop-84 [20], and previously unpublished data).

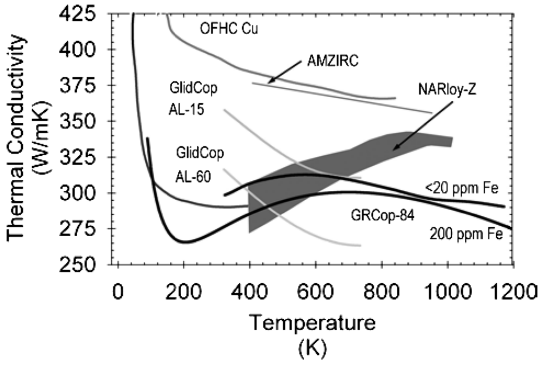

Fig. 6 Thermal conductivity of candidate liner alloys (OFHC Cu [8], NARloy-Z [8,13,21], GlidCop AL-15 [13], GlidCop AL-60 [22], AMZIRC [8], GRCop-84 [20] and previously unpublished data.

unaffected by temperature between room temperature and 600°C (1112°F) and were not statistically significantly affected by the braze cycle. Only processing had a statistically significant effect, and that effect was fairly small.

Thermal expansion is important for a liner application, because it causes thermally induced stresses that lead to creep and determines the total strain range for LCF. The thermal expansion of several of the alloys is shown in Fig. 5. Most of the candidate alloys fall within a very narrow band of thermal expansions that are approximately the same as pure copper. GRCop-84, with its 14 volume percent Cr_2Nb, has a much lower thermal expansion. Comparing averages, the thermal expansion of GRCop-84 is about 15% lower than the other alloys at 500°C (932°F).

Figure 6 shows the thermal conductivity of the candidate liner alloys. Copper has the highest conductivity, and lightly alloyed AMZIRC is barely less conductive than copper. The thermal conductivity of GlidCop is highly dependent on the volume fraction of alumina. AL-15 has an intermediate thermal conductivity, whereas AL-60 tends to be at the low end. This large decrease in thermal conductivity is the main reason GlidCop AL-15 is normally preferred.

NARloy-Z has an intermediate thermal conductivity that improves when the alloy is heated from room temperature to the anticipated hot wall temperature.

GRCop-84 has one of the lower thermal conductivities, but recent improvements in powder production to remove iron has increased the low temperature (less than 350°C or 662°F) thermal conductivity. Compared with pure copper, GRCop-84 retains more than 75% of the thermal conductivity of pure copper above room temperature.

The lower thermal conductivity is a concern, but analysis of nonoptimized liner designs in which GRCop-84 is directly substituted for NARloy-Z with no reduction in wall thickness conducted by the Rocketdyne Division of Boeing under a NASA contract has shown that the hot wall temperature will only increase 6 to 28°C (10 to 50°F). GRCop-84 can generally operate at

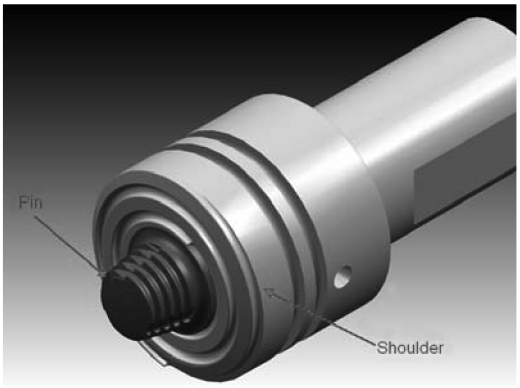

Fig. 7 Friction stir welding pin tool.

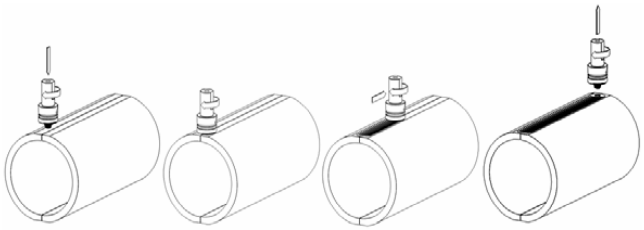

Fig. 8 Friction stir welding process.

temperatures up to 200°C (360°F) greater than NARloy-Z, and so this increase is well within the temperature capabilities of the new alloy. If the wall can be thinned to take advantage of the superior mechanical properties of GRCop-84, the hot wall temperature can actually be decreased, even with the lower thermal conductivity GRCop-84.

II. Friction Stir Welding Process Background

Friction stir welding is a solid-state welding process that uses a nonconsumable rotating pin tool to make linear welds. Typical pin tools consist of a cylindrical "shoulder" and a smaller diameter protruding "pin" (see Fig. 7). The process, shown schematically in Fig. 8, is initiated by plunging the rotating pin tool into a weld joint until the shoulder is in intimate contact with the surface of the work piece (Fig. 8a). After the pin tool has reached its final plunge depth, a dwell time is initiated wherein the material surrounding the pin tool is heated by friction and plastic deformation (Fig. 8b). Travel is initiated after sufficient dwell time, and the weld is created by literally stirring plasticized material together under compressive forces generated by the tool shoulder (Fig. 8c). Finally, the weld is concluded by halting travel and withdrawing the rotating pin tool from the work piece (Fig. 8d). It should be noted that a hole is left at the end of the weld when the pin tool is withdrawn, which can be removed in final machining.

Friction stir welding is well suited for GRCop-84, because no melting occurs. Because of this, the Cr_2Nb strengthening elements in GRCop-84 do not go into solution during welding. Also, heat-affected zone width and grain growth due to localized heating are minimized. In fact, there is significant grain refinement in the "stir zone" or "nugget" of the weld. Figure 9 shows a typical macrostructure of a friction stir weld in GRCop-84.

To date, the limited availability of GRCop-84 plate material has hindered the development of a statistically significant friction stir welding mechanical properties database. However, room-temperature tensile testing completed thus far is extremely promising. Table 1 shows all tensile data collected to date from weld development panels. Note that these data were collected from friction stir welds in both 1.27-cm (0.5-in.) thick and 1.88-cm (0.75-in.) thick rolled and annealed GRCop-84 plate material. Both "round bar" and

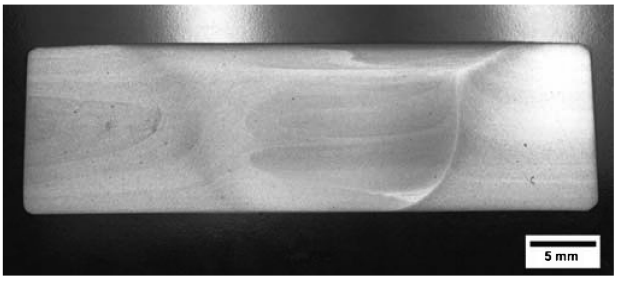

Fig. 9 Typical short-transverse macrostructure of a friction stir weld in GRCop-84.

"dog bone" types of specimens were used. Of note is the fact that average yield strength is 88% of the extruded material strength, and average ultimate tensile strength is 95% of the extruded material strength. These are respectable numbers considering that welding parameters have not yet been optimized.

III. Processing Welded Combustion Chamber Liners

As mentioned previously, GRCop-84 was designed for rapid solidification processing. On a commercial scale, the best option was conventional argon gas atomization. Scale-up work was done with Crucible Research of Pittsburgh, Pennsylvania to produce up to 727 kg (1600 lb) in a single atomization campaign. All powder was handled under argon or vacuum throughout production to minimize oxygen contamination. The powder was screened to ASTM-140 mesh (less than 106 μm). The powder was placed in a 38.4-cm (15.1 in.) diameter copper extrusion can. The can was evacuated while being heated and then sealed when a hard vacuum was obtained.

The extrusion was done at HC Starck in Coldwater, Michigan. The can was extruded to a 7.4×25.1 cm (2.9×9.9 in.) rectangular cross section. The reduction in area was 6.2:1. Modeling by Deformation Control Technologies showed that nearly full consolidation was obtained before the breakthrough of the can during extrusion. The extruded product showed no visible porosity and considerable evidence of material flow.

For rolling, the extrusions were flattened, inspected, and cut to length. The upper and lower surfaces, corresponding to the two largest faces, were machined to remove all copper from the extrusion can. This typically reduced the thickness to 6.4 cm (2.5 in.). The remaining copper extrusion can on the other faces was not removed, because it would be trimmed from the plate after rolling.

Table 1 Room-temperature tensile data

	0.2% yield, ksi	0.2% yield, Mpa	UTS, ksi	UTS, Mpa	Elongation, %
1 P7-1	29.7	204.8	58.3	402.1	19.0
2 P7-4	29.0	199.9	58.4	402.9	20.7
3 P10-1	29.2	201.3	58.5	403.6	18.3
4 P10-4	30.8	212.3	58.9	406.0	17.2
5 P11-1	28.7	197.9	58.4	402.9	16.4
6 P11-4	29.8	205.4	58.5	403.2	16.4
P12-RT2	30.3	208.9	59.9	413.1	15.4
P12-RT3	29.9	206.3	59.7	411.4	19.2
P12-RT4	30.6	210.9	56.5	410.3	18.8
P12-RT5	29.7	204.6	59.0	407.0	18.6
P12-RT6	28.9	199.1	59.1	407.2	16.3
P19-T3	29.4	202.9	58.0	399.7	18.8
P19-T4	28.6	197.1	57.5	396.7	18.6
P19-T5	28.8	198.5	56.8	391.6	16.3
Mean	29.5	203.6	58.6	404.1	17.9
S.D.	0.7	4.9	0.8	5.7	1.5
Extruded material	33.5	231.4	61.8	426.1	21.4
Joint efficiency, %	88.1		94.9		83.4

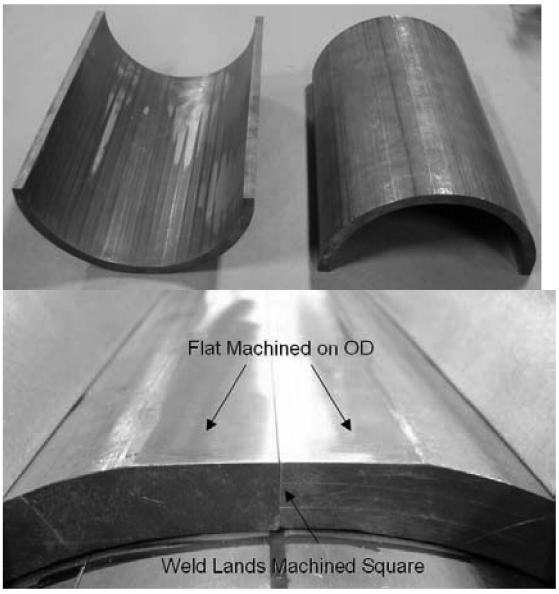

Fig. 10 Bump-formed and machined half cylinders before welding.

Warm rolling of the extruded material to plate was done at HC Starck in Euclid, Ohio. A slightly elevated temperature was used to allow some recovery and even recrystallization and avoid failure of the material observed after cold reductions of approximately 30% in previous rolling work. The extrusions were rolled to a thickness of 1.27 cm (0.5 in.) and annealed to remove any residual stress and achieve a fully recrystallized microstructure.

The plates were cut to the desired length for the cylinders. The half cylinders were made by bump forming the plates, working from the center of the plate outwards. Once the desired inner radius was obtained, the extra material was cut off and the ends machined to give a tight fit and uniform thickness. After forming, the abutting weld lands were machined square and a flat was machined onto the outside diameter at each joint to assure good contact between the pin tool shoulder and part depicted in Fig. 10.

Welding of the preforms took place on a vertical weld tool (VWT). A special fixture was fabricated to accommodate welding of the cylinders. The fixture is water-cooled to prevent excessive heat buildup and/or distortion during welding and also features a removable/replaceable anvil insert. Figure 11 shows a cylinder fixtured and ready to weld. Figure 12 shows the fixture and cylinders during welding.

The pin tool used for welding (see Fig. 7) GRCop-84 consisted of a Stellite alloy 6B body and MAR-M-246 alloy pin. Stellite 6B was selected for the shoulder body because of its excellent wear resistance at elevated temperatures. MAR-M-246 was selected as the pin alloy because of its elevated temperature strength and toughness. MAR-M-246 also has good resistance to the rubbing-type wear the pin encounters during friction stir welding.

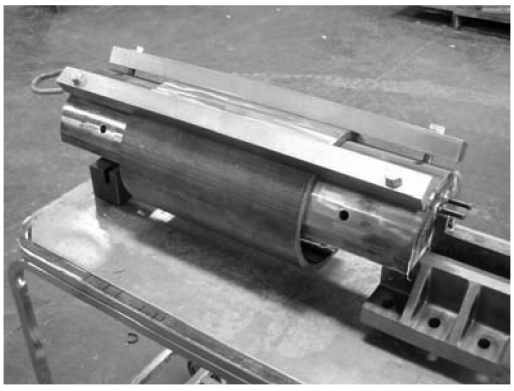

Fig. 11 Cylinder welding fixture with clamps.

Fig. 12 Fixture mounted during welding.

The geometry of the shoulder (e.g., the scroll cut) was developed to allow welding without using a lead angle. This helps to reduce and eliminate the flashing, undercut, and weld-bead concavity common to conventional smooth-shouldered friction stir welding tools.

The pin was tapered along its length and included both threads and flutes to enhancing stirring of material. This geometry was developed to reduce traverse loads, thus increasing pin life and reducing wear. The diameter of the pin was selected such that no plastic deformation of the pin would occur under welding temperatures and loads. Any plastic deformation of the pin will lead to low-cycle fatigue problems. The length of the pin was selected such that during welding there would be a 0.75-mm (0.030-in.) gap (penetration ligament) between the tip of the pin and anvil. It was shown that with a 0.75-mm (0.030-in.) gap, this pin tool is capable of achieving a full-penetration weld.

After the preforms were fixtured and mounted in the VWT, the entire volume containing the fixture and preform was purged with a mixture of argon and helium. This was done to prevent oxidation during welding. An oxygen analyzer was plumbed into the purge chamber, and oxygen content was monitored before, during, and after welding. Welding did not commence until less than 1% oxygen was present in the purged volume. The purge was not broken until 10 min (minimum) after welding, to allow the preform to cool below its oxidation temperature.

A partial-penetration tack weld was then made along the entire length of the joint. This was done using a pin tool with a pin length of approximately 2.5 mm (0.100 in.). Figure 13 shows the pin tools used; the tack tool is on the right. The purpose of this tack weld was to reduce the clamping forces necessary during full-penetration welding. Significant transverse loads (perpendicular to the direction of travel) were observed during the full-penetration pass. Without tack welding, it is very likely that the abutted joint would spread apart, forming a gap. The pin and shoulder of the full-penetration tool were sized such that the entire tack weld region was consumed during the full-penetration pass.

After tacking, a hole was predrilled at the location at which the full-penetration pin tool would plunge into the cylinder. The hole was approximately half the nominal diameter of the pin and half the material thickness in depth. The primary purpose of this hole was to act as a pilot for the pin, relieving some of the plunge loads and also preventing the tool from walking around on the cylinder. In addition, the hole reduced the amount of material displaced by the pin during the plunging process, thus reducing the amount of heating that takes place during the plunge. Before implementing the use of a predrilled hole for welding GRCop-84, there was a significant problem associated with excessive heat buildup during plunge. This excessive heat buildup significantly altered welding characteristics during the early part of the weld.

Fig. 13 Pin tools used for welding 1.27-cm (0.5-in.) thick GRCop-84; tack tool on the right, full-penetration tool on the left.

Fig. 14 Cylinders completed after welding.

Finally, the full-penetration weld pass was made. The key parameters that must be controlled during friction stir welding are 1) rotation speed (rpm): the rotating speed of the pin tool; 2) travel speed (ipm): the speed at which the pin tool traverses along the weld joint; and 3) pin tool plunge depth (in.) or plunge force (lb): the depth to which the shoulder plunges below the surface of the work piece.

Early in the development of parameters for welding the cylinders, it became apparent that the welding process put heat energy into the part and fixture faster than the water-cooling system could reject it. This was significant, because it meant that when welding parameters (rpm, ipm, and load) were fixed, the process would never reach a steady-state condition, because the power input by the process was always higher than the power taken out by the cooling system. To address this issue, the welding parameters were tapered from hotter to colder along the length of the weld. In other words, the linear (along the length of the weld) heat input was reduced by the process to compensate for the linear increase in work piece temperature. This "tapered parameter" technique proved to be very successful at producing consistent weld results.

To date, three cylinders have been welded: two 22-cm (8.66-in.) i.d. and one 13.8-cm (5.45-in.) i.d. (Fig. 14). All welds completed have been free of radiographic indications or weld defects. The first welds made had undercut that was deemed acceptable. Subsequent welds were made with tapered welding parameters and this undercut was eliminated.

Following welding and inspection, the cylinders were annealed at 600°C for 30 min, and the trim region of the cylinders was determined by referencing radiographs. The ends of the cylinder must be trimmed, because the friction stir weld does not consume the entire length of the joint. Approximately 2.54 to 3.81 cm (1 to 1.5 in.) must be trimmed from both ends.

The cylinders were then shipped to Spintech for spin forming into the characteristic hourglass shape of a combustion chamber liner. The cylinder was to be spun formed to an hourglass configuration, leading to the final configuration of combustion chamber liners following the sequence of operations shown in Fig. 15. The cylinder preforms were first mounted to a mandrel to form the smaller diameter end and move material thickness. Following this operation, the cylinder is mounted to a mandrel of the final configuration to achieve the hourglass shape.

After the initial spin-forming operation, the friction stir welded material showed no visual evidence of separation or cracking. The forming temperature was held at 760°C using a technique shown in Fig. 16. The GRCop-84 material spun formed very similarly to NARloy-Z. It was determined that GRCop-84 cylinders with friction stir welds are capable of being spun formed to a combustion chamber

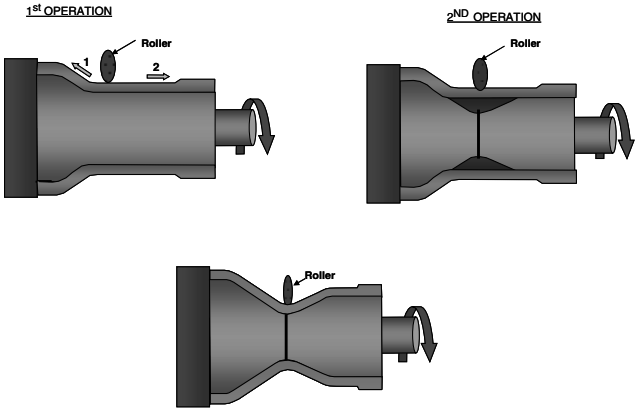

Fig. 15 Spin-forming sequence of operations to create an hourglass shape.

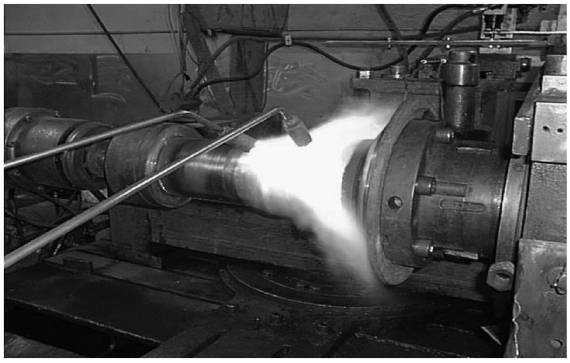

Fig. 16 Preheating cylinder preform for forming operation.

Fig. 17 Spun-formed liner before finish machining.

configuration, as shown in Fig. 17. Following the spin-forming operation, the liners will be ultrasonically inspected and either sectioned for metallurgical evaluation and mechanical property testing or machined and hot-fire tested by Boeing Rocketdyne.

IV. Conclusions

GRCop-84 exhibits properties well suited for use in a regeneratively cooled rocket engine liner. Production of the alloy has been successfully scaled up to produce powder in sufficient quantities for full-scale hardware. The alloy was successfully extruded, rolled, formed, and welded into a subscale combustion chamber liner suitable for hot-fire testing.

The friction stir weld process is well suited for GRCop-84. The solid-state joining method produces welds with mechanical properties that are 96% of the parent metal properties.

Acknowledgments

The authors would like to acknowledge the Next Generation Launch Technology program for funding this work. This manufacturing demonstration could not have been accomplished without the contributions of Crucible Research for producing the powder, H.C. Stark for extruding and rolling the plate, and Boeing Rocketdyne for testing the spun-form liners.

References

[1] Ellis, D. L., and Dreshfield, R. L., "Preliminary Evaluation of a Powder Metal Copper-8 Cr-4 Nb Alloy," *Proceedings of the Advanced Earth-to-Orbit Conference*, Vol. 1, NASA Marshall Space Flight Center, Huntsville, AL, May 1992, pp. 18–27; also NASA CP-3174.

[2] Ellis, D. L., Dreshfield, R. L., Verrilli, M. J., and Ulmer, D. G., "Mechanical Properties of a Cu-8 Cr-4 Nb Alloy," *Proceedings of the Advanced Earth-to-Orbit Conference*, Vol. 1, NASA Marshall Space Flight Center, Huntsville, AL, May 1994, pp. 32–41; also NASA CP-3282, .

[3] Shapiro, E., and Crane, J., "Optimizing Conductivity, Formability and Relaxation Resistance in Copper Alloys," *High Conductivity Copper and Aluminum Alloys*, edited by E. Ling, and, P. W. Taubenblat, The Metallurgical Society of AIME (TMS/AIME), Warrendale, PA, 1984, pp. 53–62.

[4] Ashby, M. F., *Oxide Dispersion Strengthening: Second Bolton Landing Conference*, Gordon and Breach, New York, 1968, p. 143.

[5] Grant, N.J., Cline, C.F., Davis, L.A., Kear, B.H., and Luborsky, F.E., "Amorphous and Metastable Microcrystalline Rapidly Solidified Alloys: Status and Potential," National Materials Advisory Board, Rept. NMAB-358, Washington, D.C., May 1980.

[6] Ellis, D. L., "Precipitation Strengthened High Strength, High Conductivity Cu-Cr-Nb Alloys Produced By Chill Block Melt Spinning," Ph.D. Dissertation, Case Western Reserve Univ., Cleveland, OH, 1989; also NASA CR-185114.

[7] Stephens, J. J., Bourcier, R. J., Vigil, F. J., and Schmale, D. T., "Mechanical Properties of Dispersion Strengthened Copper: A Comparison of Braze Cycle Annealed and Coarse Grained Microstructures," Sandia National Labs, Rept. 88-1351, Albuquerque, NM, Sept. 1988.

[8] Anon., "Thrust Chamber Life Prediction, Vol. 1: Mechanical and Physical Properties of High Performance Rocket Nozzle Materials," NASA CR-134806, Mar. 1975.

[9] Schmidt, E. H., "Mechanical Property Data for Oxygen-Free High-Conductivity Copper and Boron Deoxidized Copper," NASA 66-10273, Feb. 1966.

[10] Nagai, T., Henmi, Z., and Koda, S., "Annealing Behavior of Copper-Chromium, Copper-Zirconium and Copper-Zirconium-Chromium Alloys," *Journal of the Japan Copper and Brass Research Association*, Vol. 14, No. 1, 1975, pp. 60–73; also Copper Development Association, Extract 13298, New York.

[11] Horn, D. D., and Lewis, H. F., "Property Investigation of Copper-Base Alloys at Ambient and Elevated Temperatures," Arnold Engineering Development Center, Rept. TR-65-72, Arnold Air Force Station, TN, July 1965.

[12] Nadkarni, A. V., "Dispersion Strengthened Copper Properties and Applications," *High Conductivity Copper and Aluminum Alloys*, edited by E. Ling, and P. W. Taubenblat, The Metallurgical Society of AIME (TMS/AIME), Warrendale, PA, 1984, pp. 53–62.

[13] Ellis, D. L., and Michal, G. M., "Mechanical and Thermal Properties of Two Cu-Cr-Nb Alloys and NARloy-Z," NASA CR-198529, Oct. 1996.

[14] Polák, J., Obrtlík, K., Hájek, M., and Vašek, A., "Cyclic Stress-Strain Response of Polycrystalline Copper in a Wide Range of Plastic Strain Amplitudes," *Materials Science and Engineering, A*, Vol. 151, No. 1, Apr. 1992, pp. 19–27.

[15] Anon., "Thrust Chamber Life Prediction, Vol. 1: Mechanical and Physical Properties of High Performance Rocket Nozzle Materials," NASA CR-134806, Mar. 1975.

[16] Conway, J. R., Stentz, R. H., and Berling, J. T., "High-Temperature, Low-Cycle Fatigue of Advanced Copper-Base Alloys for Rocket Nozzles, Part 2: NASA 1.1, Glidcop, and Sputtered Copper Alloys," NASA CR-134628, Nov. 1974.

[17] Conway, J. R., Stentz, R. H., and Berling, J. T., "High-Temperature, Low-Cycle Fatigue of Advanced Copper-Base Alloys for Rocket Nozzles, Part 1: NARloy-Z," NASA CR-134627, May 1974.

[18] Nguyentat, T., Gibson, V. A., and Horn, R. M., "NASA-Z: A Liner Material for Rocket Combustion Chambers," AIAA/SAE/ASME 27th

Joint Propulsion Conference, Sacramento, CA, AIAA Paper 91-2487, 1991.

[19] Williams, L. R., Young, J. D., and Schmidt, E. H., "Design and Development Engineering Handbook of Thermal Expansion Properties of Aerospace Materials at Cryogenic and Elevated Temperatures," Rocketdyne Div. Contract No. NAS-8-19, Mar. 1967.

[20] Ellis, D. L., and Keller, D. J., "Thermophysical Properties of GRCop-84," NASA CR-2000-210055, NASA Glenn Research Center, Cleveland, OH, May 2003.

[21] Siu, M. C. I., Carroll, W. L., and Watson, T. W., "Thermal Conductivity and Electrical Resistivity of Six Copper Base Alloys," National Bureau of Standards, Rept. NBSIR 76-1003, Mar. 1976.

[22] Groza, J., "Heat Resistant Dispersion Strengthened Copper Alloys," *Journal of Materials Engineering and Performance*, Vol. 1, No. 1, Feb 1992, pp. 113–121.

T. Wang
Associate Editor